MOLECULAR PHARMACOLOGY
Vol. 77, No. 2
59675/3554906
Printed in U.S.A.

Mol Pharmacol 77:195–201, 2010

Aryl Hydrocarbon Receptor Regulates Cell Cycle Progression in Human Breast Cancer Cells via a Functional Interaction with Cyclin-Dependent Kinase 4

Melissa A. Barhoover, Julie M. Hall, William F. Greenlee, and Russell S. Thomas

The Hamner Institutes for Health Sciences, Research Triangle Park, North Carolina

Received July 22, 2009; accepted November 16, 2009

ABSTRACT

The aryl hydrocarbon receptor (AHR) is a ligand-activated transcription factor with constitutive activities and those induced by xenobiotic ligands, such as 2,3,7,8-tetrachlorodibenzo-*p*-dioxin (TCDD). One unexplained cellular role for the AHR is its ability to promote cell cycle progression in the absence of exogenous ligands, whereas treatment with exogenous ligands induces cell cycle arrest. Within the cell cycle, progression from G_1 to S phase is controlled by sequential phosphorylation of the retinoblastoma protein (RB1) by cyclin D–cyclin-dependent kinase (CDK) 4/6 complexes. In this study, the functional interactions between the AHR, CDK4, and cyclin D1 (CCND1) were investigated as a potential mechanism for the cell cycle regulation by the AHR. Time course cell cycle and molecular experiments were performed in human breast cancer cells. The results demonstrated that the AHR and CDK4 interact within the cell cycle, and the interaction was disrupted upon TCDD treatment. The disruption was temporally correlated with G_1 cell cycle arrest and decreased phosphorylation of RB1. Biochemical reconstitution assays using in vitro-translated protein recapitulated the AHR and CDK4 interaction and showed that CCND1 was also part of the complex. In vitro assays for CDK4 kinase activity demonstrated that RB1 phosphorylation by the AHR/CDK4/CCND1 complex was reduced in the presence of TCDD. The results suggest that the AHR interacts in a complex with CDK4 and CCND1 in the absence of exogenous ligands to facilitate cell cycle progression. This interaction is disrupted by exogenous ligands, such as TCDD, to induce G_1 cell cycle arrest.

The aryl hydrocarbon receptor (AHR) is a ligand-activated transcription factor and a member of the basic helix-loop-helix, period/aryl hydrocarbon receptor nuclear translocator (ARNT)/single-minded (PAS) superfamily. In the canonical model for AHR signaling, the unliganded form of the receptor exists in the cytoplasm in a stable complex with HSP90, the AHR-interacting protein, and PTGES3 (Petrulis and Perdew, 2002). After ligand binding, the AHR translocates to the nucleus and binds with ARNT. The AHR/ARNT heterodimer binds to xenobiotic response elements and regulates a diverse set of genes (Poland and Knutson, 1982; Hankinson, 1995; Kolluri et al., 1999; Thomsen et al., 2004; Hsu et al., 2007). Although it is widely believed that the majority of biological effects resulting from AHR ligand activation are driven through direct binding to xenobiotic response elements (Bunger et al., 2008), regulation of the AHR effects through protein interactions and other nongenomic mechanisms have been proposed as an important route of AHR activity. For example, ligand activation of the AHR has been shown to induce proteosome degradation of estrogen receptor α, thereby reducing the ability of the cell to respond to estrogens (Wormke et al., 2003). In addition, the AHR can repress acute-phase gene expression by inhibiting the recruitment of RELA and CEBPB to the promoters of target genes (Patel et al., 2009). Other nongenomic effects of the AHR have been proposed in regulating the CUL4B (Ohtake et al., 2009), mitogen-activated protein kinase (Tan et al., 2002), protein kinase A (Dong and Matsumura, 2009), and SRC (Dong and Matsumura, 2009; Haarmann-Stemmann et al., 2009) signaling pathways.

There is considerable evidence indicating that the AHR plays a role in regulating cell growth (Hahn et al., 2009). Early studies using the AHR-deficient variant of the mouse

This work was supported by The Hamner Pilot Projects Initiative, The Hamner Institutes for Health Sciences.

Article, publication date, and citation information can be found at http://molpharm.aspetjournals.org.

doi:10.1124/mol.109.059675.

ABBREVIATIONS: AHR, aryl hydrocarbon receptor; ARNT, aryl hydrocarbon nuclear translocator; CDK4, cyclin-dependent kinase 4; ER−, estrogen receptor negative; ER+, estrogen receptor positive; TCDD, 2,3,7,8-tetrachlorodibenzo-*p*-dioxin; RB1, retinoblastoma protein; CCND1, cyclin D1; FBS, fetal bovine serum; C/D FBS, charcoal-stripped fetal bovine serum; E2, 17-β-estradiol; HSP90, 90-kDa heat shock protein; DMSO, dimethyl sulfoxide; DMEM, Dulbecco's modified Eagle's medium; PAGE, polyacrylamide gel electrophoresis; PVDF, polyvinylidene difluoride; PCR, polymerase chain reaction; IP, immunoprecipitation; ECL, enhanced chemiluminescence; MEM, minimal essential medium.

Hepa1c1c7 cell line identified an increased doubling time and prolonged G_1 progression compared with the wild-type cell line (Ma and Whitlock, 1996). In addition, cell cycle progression of murine or human hepatoma cells from G_1 to S is prolonged by transfection of antisense cDNA or small interfering RNA targeting the AHR (Ma and Whitlock, 1996; Abdelrahim et al., 2003). These and other studies suggest a role for the AHR in facilitating progression through G_1 in the absence of an exogenous ligand. In a seemingly contradictory role, treatment with the exogenous AHR ligand 2,3,7,8-tetrachlorodibenzo-*p*-dioxin (TCDD) inhibited DNA synthesis in rat primary hepatocytes and in the 5L rat hepatoma cell line (Hushka and Greenlee, 1995). In the 5L rat hepatoma cell line, the inhibition of proliferation by TCDD was linked to G_1 cell cycle arrest (Hushka and Greenlee, 1995; Weiss et al., 1996; Elferink et al., 2001).

To date, no unifying model exists that explains the apparent contradictory roles of the AHR in the cell cycle. However, multiple models have been proposed to explain the mechanism of G_1 arrest by the ligand-activated AHR. The generally accepted model holds that in an unliganded state, HSP90 binding masks the LXCXE motifs within the Per/ARNT/Sim domain of the AHR (Elferink et al., 2001). Upon ligand binding, the AHR sheds HSP90, translocates to the nucleus, and performs two separate functions that lead to G_1 arrest. First, the ligand-bound AHR interacts with a hypophosphorylated RB1 (Ge and Elferink, 1998; Puga et al., 2000; Elferink et al., 2001). The interaction of the ligand-bound AHR with RB1 inhibits the recruitment of EP300 and maintains its interaction with E2F, resulting in the repression of cell cycle progression genes (Marlowe et al., 2004). Second, the ligand-bound AHR interacts with ARNT and stimulates the transcription of the cell cycle inhibitory protein CDKN1B (p27Kip1) (Kolluri et al., 1999). Together, the nongenomic and genomic roles of the ligand-activated AHR result in cell cycle arrest.

Advancement through G_1 of the cell cycle is primarily regulated by RB1. The active, hypophosphorylated RB1 arrests cells in G_1 through repressive interactions with E2F and the inhibition of genes involved in cell cycle progression (Flemington et al., 1993). Entry into S phase occurs after RB1 inactivation by cyclin D-CDK4/6 mediated hyperphosphorylation (Kato et al., 1993). The present study investigated the functional interactions between the AHR, CDK4, and CCND1 as a potential mechanism for the AHR-mediated cell cycle effects. The results show that AHR, CDK4, and CCND1 physically interact in the absence of exogenous ligands. The interaction is disrupted after treatment with TCDD, and the disruption was temporally correlated with G_1 cell cycle arrest and decreased phosphorylation of RB1. The AHR/CDK4 interaction and its disruption by TCDD was confirmed using biochemical reconstitution assays. In vitro assays for CDK4 kinase activity also demonstrated that RB1 phosphorylation by the AHR/CDK4/CCND1 complex was reduced in the presence of TCDD.

Materials and Methods

Chemicals. TCDD ($C_{12}H_4Cl_4O_2$) was purchased from AccuStandard (New Haven, CT). Dimethyl sulfoxide (DMSO; Me_2SO_4) and (17β)-estra-1,3,5(10)-triene-3,17-diol (17β-estradiol, E2; $C_{18}H_{24}O_2$) was purchased from Sigma-Aldrich (St. Louis, MO).

Cell Lines and Growth Conditions. Two human breast cancer cell lines were used in this study: the estrogen receptor-negative (ER−) cell line MDA MB-231; and the estrogen receptor-positive (ER+) cell line MCF-7. Both cell lines were maintained in a 50:50 mixture of Dulbecco's modified Eagle's medium and Ham's F-12 with L-glutamine (DMEM/Ham's F-12; 50:50) (Mediatech, Manassas, VA). The media were supplemented with 8% fetal bovine serum (FBS), 1% 100× MEM nonessential amino acids, and 1% 100× MEM sodium pyruvate solution (Invitrogen, Carlsbad, CA). The cells were maintained in a humidified environment at 37°C and 5% CO_2. Before experiments, cells were split into DMEM/Ham's F-12 50:50 without phenol red (Mediatech) and supplemented with 8% charcoal-stripped FBS (C/D FBS) (HyClone, Logan, UT), 1% 100× MEM nonessential amino acids, and 1% 100× MEM sodium pyruvate solution. For cell cycle and coimmunoprecipitation experiments, cells were synchronized for 24 h in DMEM/Ham's F-12 50:50 without phenol red and supplemented with 0.2% C/D FBS and 1% 100× HEPES (Invitrogen). When specified, cells were treated with TCDD to a final concentration of 10 nM. Control cells were treated with an equal volume of the DMSO vehicle (0.1% of the total volume).

Cell Cycle Experiments. The MDA MB-231 and MCF-7 cell lines were plated in six-well culture dishes in phenol red-free media at a density of 0.1×10^6 cells/ml. For the synchronized cell studies, the cells were allowed to incubate overnight before serum starvation in 0.2% C/D FBS media for 24 h. The cells were then stimulated with 8% C/D FBS medium and treated with 10 nM TCDD or DMSO vehicle. For asynchronous cell studies, cells were allowed to incubate overnight after plating, and then the media were changed to treated medium as mentioned above. E2 was also added to the media of MCF-7 treated and control cells. After treatment, cells were fixed in 70% ethanol at the indicated time points and stored at 4°C for cell cycle analysis. For the dose-response studies, synchronized cells were treated with 0.1, 0.3, 3, or 10 nM TCDD or DMSO vehicle and harvested at the 24-h time point. Cells were stained with Guava Cell Cycle reagent (Guava Technologies, Hayward, CA) according to the manufacturer's instructions. Cell cycle data were obtained using the Guava Personal Cell Analysis System (Guava Technologies). A total of three experimental replicates in each cell line were performed.

Cellular Coimmunoprecipitation and Western Blotting. The MDA MB-231 and MCF-7 cell lines were plated at a cell density of 1.0×10^6 cells/ml in 100-mm cell culture plates. The cells were treated simultaneously with the cell cycle experiments as described above. At the indicated time points, cells were harvested by scraping in ice-cold phosphate-buffered saline. Cells were pelleted and stored at −80°C until analysis was performed. Cells were lysed in 1 ml of Mammalian Protein Extraction Reagent (Thermo Fisher Scientific, Waltham, MA) supplemented with 1% 100× Halt Protease Inhibitor Single-Use Cocktail (Thermo Fisher Scientific). The total protein concentration was measured based on the absorbance at 260 nm. For Western blot experiments, 10 to 50 μg of total protein per sample was analyzed by SDS-PAGE and transferred to PVDF as described above. The membranes were probed with α-phospho-RB1 (Ser780) antibody (Cell Signaling Technology, Danvers, MA). An antibody for β-actin (Santa Cruz Biotechnology, Santa Cruz, CA) was used as a loading control. For the coimmunoprecipitation experiments, 500 to 1000 μg of total protein per sample was allowed to incubate overnight with 2 μg of antibody, α-CDK4 (DCS-35) (Santa Cruz Biotechnology), or a negative control α-GAL4 (DNA binding domain) (N-19) (Santa Cruz Biotechnology). The antibody-bound protein was incubated with 50 μl of Immobilized Protein A/G resin (Pierce, Rockford, IL) for 2 h while rotating at ambient temperature. The immobilized Protein A/G resin was washed four times by adding 1 ml of BupH Tris-buffered saline (IP buffer) (Pierce) and centrifuged at 2500*g* for 5 min. The supernatant was then discarded. The complex-bound Protein A/G resin was washed with 1 ml of deionized water, centrifuged at 2500*g* for 5 min, and the supernatant was discarded. Electrophoresis loading buffer (Pierce) was added to the complex-bound protein A/G resin, incubated at 95°C for 5 min, and centrifuged at 2500*g* for 5 min. The supernatant was separated by

SDS-PAGE on an 8% Tris-glycine gel (Invitrogen). The gel was transferred to PVDF membrane (Bio-Rad Laboratories, Hercules, CA) and probed with α-AHR (N-Term) (Zymed, San Francisco, CA) followed by ECL detection (GE Healthcare, Chalfont St. Giles, Buckinghamshire, UK). For densitometry, the films were scanned on the Bio-Rad Versa-Doc Imaging System, and the acquired images were analyzed for band density using Bio-Rad's PD Quest 2-D analysis software.

In Vitro Transcription/Translation. Plasmids were constructed using polymerase chain reaction (PCR) and the Gateway system (Invitrogen). Primers were designed for the AHR, CDK4, and CCND1 with DNA recombination sequences (*att* sites) flanking the open reading frames. The primers were as follows: AHR, 5′-**GGGGACAAGTTTGTACAAAAAAGCAGGCTTCGAAGGAGATAGAACCATGG**GAGGCAGCAGCAGCGCCAACATCACC-3′ (forward) and 5′-**GGGGACCACTTTGTACAAGAAAGCTGGGT**CCTACAGGAATCCACTGGATGTCAAATCAGG-3′ (reverse); CDK4, 5′-**GGGGACAATGTTGTACAAAAAAGCAGGCTTCGAAGGAGATAGAACCATGG**CTACCTCTCGATATGAGC-3′ (forward) and 5′-**GGGGACCACTTTGTACAAGAAAGCTGGGT**CCTACTCCGGATTACCTTCATCC-3′ (reverse); CCND1, 5′-**GGGGACAAGTTTGTACAAAAAAGCAGGCTTCGAAGGAGATAGAACCATGG**AACACCAGCTCCTGTCG-3′ (forward) and 5′-**GGGGACCACTTTGTACAAGAAAGCTGGGT**CCTAGATGTCCACGTCCCGCACG-3′ (reverse); (boldface bases signify *att* sites). The open reading frames were amplified by PCR and cloned in the pDONR 221 entry vector (Invitrogen). The open reading frames for each gene were transferred by recombination cloning into the pcDNA3.1nV5-DEST vector (Invitrogen).

For the in vitro transcription/translation reaction, 2 μg of plasmid was used in a 50-μl in vitro TNT Quick Coupled Transcription/Translation system (Promega, Madison, WI). Reactions were incubated at 30°C for 1.5 h. Total protein concentration was determined using the Bio-Rad Protein Assay Kit (Bio-Rad) using BSA as the protein standard. Protein expression was confirmed by Western blotting, and the translated proteins were used in the complex reconstitution and kinase assays.

Biochemical Reconstitution Assays. To our knowledge, no stoichiometric studies have been performed for AHR, CDK4, and CCND1 proteins. As a result, reconstitution assays were carried out using equal amounts of protein (200 μg) based on the total protein concentration. The proteins were incubated for 30 min on ice in the presence of either 10 nM TCDD or an equal volume of DMSO vehicle (0.1% of the total reaction volume). After the incubation, 2 μg of α-CDK4 agarose conjugate (DCS-35) or α-CCND1 agarose conjugate (DCS-6) (Santa Cruz Biotechnology) was added and allowed to incubate overnight while rotating at 4°C. The complexes were washed three times with IP buffer and once with deionized water. The washed complexes were boiled for 5 min in protein loading buffer, run on an 8% Tris-glycine gel (Invitrogen), and transferred to PVDF membrane (Bio-Rad). The membrane was probed with α-AHR (N-Term) (Zymed) and detected with ECL (GE Healthcare). Densitometry was performed as described in the preceding sections.

In Vitro CDK4 Kinase Assays. Equal amounts of each protein (200 μg) were combined and allowed to form complexes on ice for 30 min. After the incubation, 2 μg of anti-CDK4 agarose conjugate (DCS-35) (Santa Cruz Biotechnology) was added and allowed to incubate overnight while rotating at 4°C. Complexes were washed with 200 μl of kinase buffer (Cell Signaling Technology). The agarose beads were pelleted and the buffer removed. The complexes were resuspended in 45 μl of kinase buffer containing ATP ($C_{10}H_{16}N_5O_{13}P_3$) (Cell Signaling Technology) to a final concentration of 0.3 mM, 2.5 μg of retinoblastoma protein ($p110^{RB}$) (QED Biosciences, San Diego, CA), and 10 nM TCDD or DMSO (0.1% of total reaction volume). Reactions were incubated for 30 min at 30°C with slow shaking. The agarose beads were pelleted, and the supernatant was removed and prepared for SDS-PAGE analysis as described below. Complexes were washed three times with IP buffer and once with deionized water. Pellets were resuspended in protein loading buffer, boiled for 5 min, separated by SDS-PAGE on an 8% Tris-glycine gel (Invitrogen), and transferred to PVDF membrane (Bio-Rad). The membrane was probed with α-RB1 (C-15) (Santa Cruz Biotechnologies) and α-phospho-RB1 (Ser780) (Cell Signaling Technology) and detected with ECL (GE Healthcare). Densitometry was performed as described in the preceding sections.

Results

AHR Ligand Activation Inhibits the Progression of ER+ and ER− Human Breast Cancer Cells at the $G_1 \rightarrow S$ Transition in the Cell Cycle. The presence of AHR protein was verified by Western blotting in both MCF-7 (ER+, PR+, HER2−) and MDA MB-231 (ER−, PR−, HER2−) breast cancer cell lines (data not shown). The biological activity of the AHR was assessed based on the induction of CYP1A1 mRNA using quantitative real-time PCR. In both cell lines, CYP1A1 mRNA was up-regulated after TCDD treatment (data not shown).

To evaluate the cell cycle effects of AHR ligand activation, time course flow cytometry measurements were performed in both MCF-7 and MDA MB-231 breast cancer cell lines after treatment with 10 nM TCDD or the DMSO vehicle. 17β-Estradiol (E2) was also added to the medium for the estrogen-dependent MCF-7 cells. The results showed that TCDD treatment resulted in G_1 arrest in both synchronous and asynchronous cells and in both cell lines (Fig. 1). For synchronous cells, neither the MDA MB-231 cells nor the MCF-7 cells treated with TCDD significantly progressed out of G_1 arrest over the 48-h time period. In contrast, only ~40% of the MDA MB-231 vehicle control cells and ~45% of the MCF-7 E2/vehicle control cells remained in G_1 arrest at the end of 48 h. For asynchronous cells, an increasing percentage of cells in G_1 was observed over the 48-h period for both cell

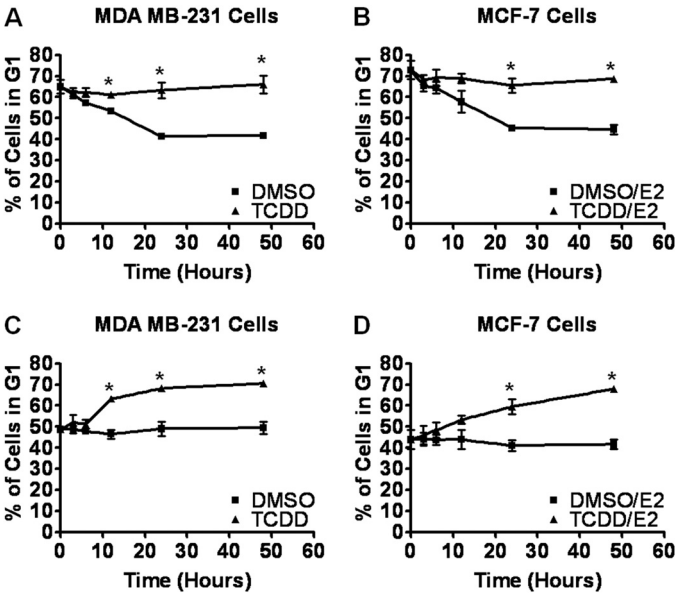

Fig. 1. TCDD induced G_1 arrest in both ER− (MDA MB-231) and ER+ (MCF-7) human breast cancer cells. Subconfluent, synchronous populations of MDA MB-231 (A) and MCF-7 (B) cells were serum-stimulated and treated with either DMSO or 10 nM TCDD. Subconfluent, asynchronous populations of MDA MB-231 (C) and MCF-7 (D) cells were treated with either DMSO or 10 nM TCDD. For both synchronous and asynchronous experiments, E2 was added to the media of MCF-7 cells. Cells were harvested at the indicated time points, fixed in ethanol, and stained with Guava Cell Cycle reagent (Guava Technologies). DNA content was determined using the Guava Personal Cell Analysis System (Guava Technologies). The data represent the mean ± S.D. from three separate experiments. *, $p < 0.05$ based on a two-sample Student's t test.

lines after treatment with TCDD. Control cells maintained a stable percentage of cells in G_1. Thus, ligand activation of the AHR inhibits cell cycle progression in both ER− and ER+ human breast cancer cell lines.

Dose-response studies of the cell cycle effects of TCDD were performed at the 24-h time point in both MCF-7 and MDA MB-231 breast cancer cell lines. In both cell lines, a dose-response trend was observed (Fig. 2). In the MDA MB-231 cells, significant G_1 arrest was observed at 0.1 nM TCDD, whereas in MCF-7 cells, significant G_1 arrest was observed at 0.3 nM.

RB1 Phosphorylation Is Decreased by TCDD. To investigate the temporal association of the TCDD-induced G_1 arrest with RB1 phosphorylation, time course Western blot analysis was performed using an RB1 phosphospecific antibody. The results show a significant increase in RB1 phosphorylation at the 24-h time point in both breast cancer cell lines treated with the DMSO vehicle (Fig. 3). A small amount of RB1 phosphorylation was present at other time points in the MDA MB-231 cells and may be due to reduced synchronization in this cell line. The extent of RB1 phosphorylation was decreased by TCDD treatment in both cell lines, and the results were temporally correlated with G_1 cell cycle arrest (Fig. 1). The TCDD-related decrease in RB1 phosphorylation is consistent with a previous study in MCF-7 cells (Wang et al., 1998).

Coimmunoprecipitation of AHR with CDK4 Is Disrupted after Treatment with TCDD. Progression from G_1 to S phase is controlled by sequential phosphorylation of RB1 by cyclin D-CDK4/6 complexes. Although previous studies have shown a physical interaction between AHR and the hypophosphorylated form of RB1 (Ge and Elferink, 1998; Puga et al., 2000; Elferink et al., 2001), no published studies have demonstrated a functional interaction with CDK4. In parallel with the cell cycle studies, time course coimmunoprecipitation experiments were performed to examine both the physical interaction between AHR and CDK4 and the ligand-dependent nature of the interaction. The results show that the AHR interacts with CDK4 in both MDA MB-231 and MCF-7 human breast cancer cells. At time 0 after synchronization, a strong interaction between AHR and CDK4 was observed in both treated and untreated cells and in both the ER+ and ER− cell lines. After treatment with TCDD, the AHR/CDK4 interaction was diminished by the 12-h time point for both cell lines (Fig. 4, A and B), and at the 24-h time point, greater than an 80% reduction was observed (Fig. 4C). The disruption of the AHR/CDK interaction temporally correlated with the decreased RB1 phosphorylation and G_1 cell cycle arrest. The data suggest that disruption of the AHR/CDK4 interaction has functional consequences within the cell cycle.

In Vitro Reconstitution of the AHR/CDK4/CCND1 Complex. To confirm the interaction between AHR and CDK4, biochemical reconstitution experiments were performed using in vitro-translated proteins. The AHR/CDK4 interaction was examined in the presence and absence of ligand and the CDK4 binding partner, CCND1. The results demonstrate that the AHR and CDK4 can form protein complexes in vitro and support the time course coimmunoprecipitation experiments in the breast cancer cells (Fig. 5). Fur-

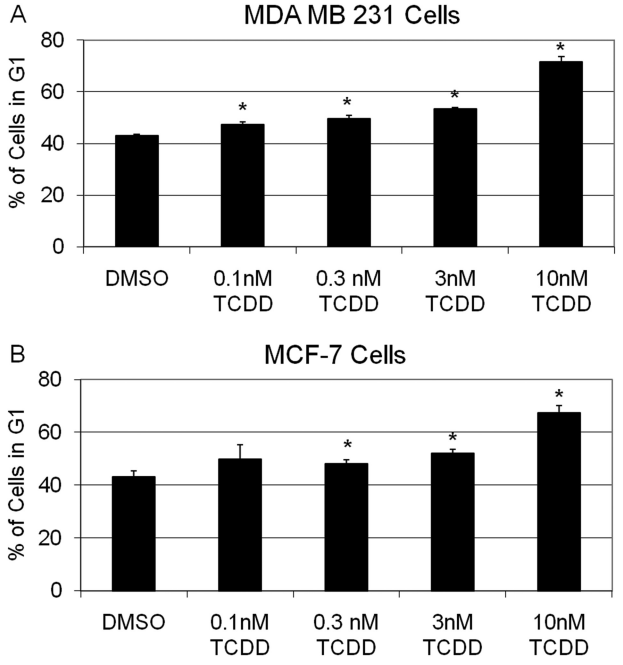

Fig. 2. Dose-response changes in G_1 arrest in both ER− (MDA MB-231) and ER+ (MCF-7) human breast cancer cells after exposure to TCDD. Subconfluent, synchronous populations of MDA MB-231 (A) and MCF-7 (B) cells were serum-stimulated and treated with either DMSO or different concentrations of TCDD. E2 was added to the media of MCF-7 cells. Cells were harvested at the 24-h time point, fixed in ethanol, and stained with Guava Cell Cycle reagent (Guava Technologies). DNA content was determined using the Guava Personal Cell Analysis System (Guava Technologies). The data represent the mean ± S.D. from three separate experiments. *, $p < 0.05$ based on a two-sample Student's t test.

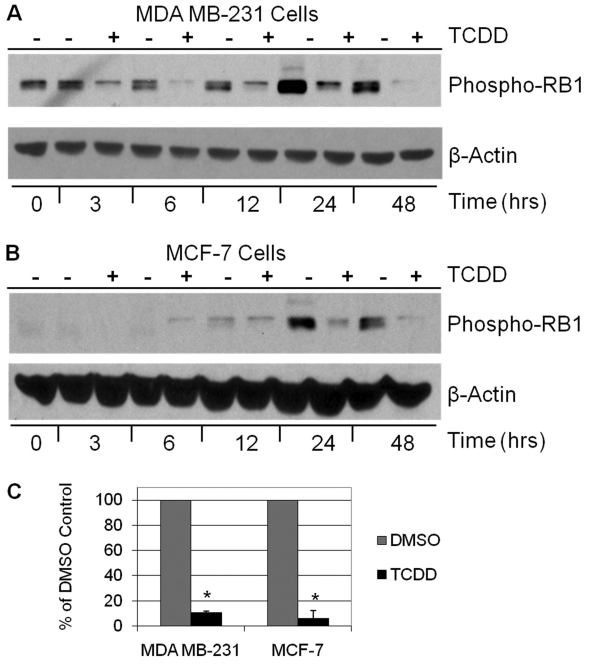

Fig. 3. TCDD decreases RB1 phosphorylation in human breast cancer cells. Subconfluent, synchronous populations of MDA MB-231 (A) and MCF-7 (B) cells were serum-stimulated in the presence of DMSO or 10 nM TCDD. E2 was added to the media of MCF-7 cells. Total cell lysates were evaluated for total RB1 phosphorylation by SDS-PAGE and Western blotting with a α-phospho-RB1 antibody. The blots are representative of three independent experiments. C, densiometric measurements on the 24-h time point and normalized as a percentage of the DMSO vehicle control. The results are mean ± S.D. from three separate experiments. *, $p < 0.05$ based on a one-sample Student's t test.

thermore, the AHR can be pulled down with both α-CDK4 and α-CCND1 antibodies, indicating that these three proteins are part of a larger complex. Treatment with the exogenous AHR ligand TCDD completely disrupts the AHR/CDK4 interaction, whereas the addition of CCND1 partially rescues the interaction. It should be noted that the actual interaction of these proteins inside cells may depend on their concentrations and relative ratios. It is possible that the conditions in the reconstitution experiments may be outside the range of the conditions existing within cells. Therefore, interpretation of the reconstitution experiments must be performed together with the cellular coimmunoprecipitation experiments.

CDK4 Kinase Activity by the AHR/CDK4/CCND1 Complex Is Inhibited by TCDD in Vitro. To evaluate the functional effects of the AHR/CDK4/CCND1 interaction, the biochemical reconstitution experiments were expanded to include the addition of RB1. The phosphorylation status of RB1 was measured using a phosphospecific antibody. The data demonstrate the ability of the AHR/CDK4/CCND1 complex to phosphorylate RB1 (Fig. 6). The extent of phosphorylation is decreased in the presence of TCDD compared with the vehicle control. To ensure that this kinase activity is specific to the protein complex, each of the proteins was assayed individually for their ability to phosphorylate RB1, and none of the proteins alone was able to phosphorylate RB1 (data not shown). The results of the kinase reconstitution experiments demonstrate that AHR/CDK4/CCND1 complex is functional and that disruption of the complex by TCDD inhibits RB1 phosphorylation.

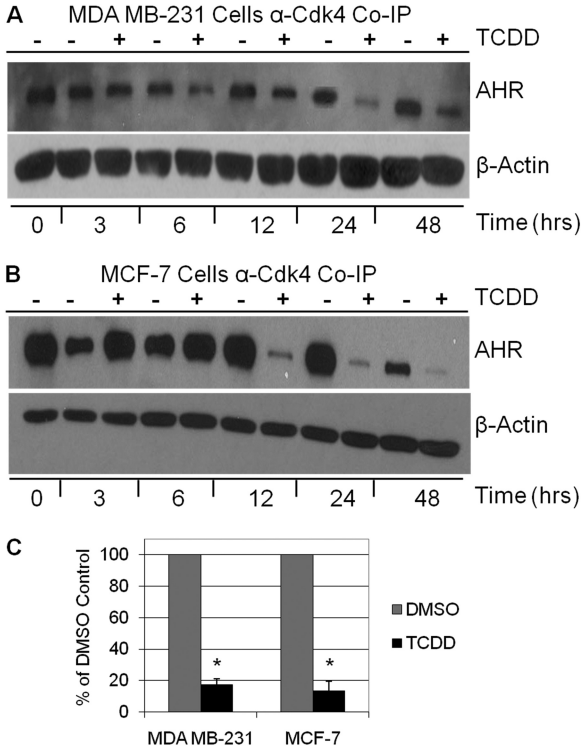

Fig. 4. The AHR associates with CDK4 in the cell cycle, and the interaction is disrupted by TCDD. Subconfluent, synchronous populations of MDA MB-231 (A) and MCF-7 (B) cells were serum-stimulated in the presence of DMSO or 10 nM TCDD. E2 was added to the media of MCF-7 cells. Cells were harvested at the indicated time points by scraping in ice-cold phosphate-buffered saline, pelleted, and frozen. Cell pellets were lysed with M-PER Mammalian Protein Extraction Reagent, and protein complexes were pulled down with anti-CDK4 agarose conjugated resin. Immunoprecipitates were analyzed by SDS-PAGE and Western blotting for AHR. The blots are representative of three independent experiments. No AHR protein was detected when an irrelevant antibody was used for the immunoprecipitation (data not shown). C, densiometric measurements on the 24-h time point and normalized as a percentage of the DMSO vehicle control. The results are mean ± S.D. from three separate experiments. *, $p < 0.05$ based on a one-sample Student's t test.

Discussion

The developmental and cancer-related effects of exposure to exogenous AHR agonists have been widely investigated. Multiple studies and review articles have attempted to link these endpoints with the known effects of AHR agonists on the cell cycle, regulation of oncogenic pathways, and interference with apoptosis (Marlowe and Puga, 2005; Ray and Swanson, 2009). Despite the multitude of studies, fundamental questions still remain regarding the role of the AHR in the cell cycle. One of these questions is how the AHR facilitates cell cycle progression in the absence of exogenous ligands, whereas exposure to exogenous ligands arrests cells in G_1. Because of the role of CDK4 and CCND1 in the G_1 to S progression of the cell cycle, the functional interaction between the AHR, CDK4, and CCND1 was investigated as a potential mechanism.

The results demonstrate that in the absence of exogenous ligands, the AHR interacts with CDK4 through the G_1 to S transition of the cell cycle, and the interaction correlates with RB1 phosphorylation. Biochemical reconstitution assays confirm that the AHR exists in a complex with CDK4 and CCND1. The reconstitution assays also demonstrate that the AHR/CDK4/CCND1 complex can phosphorylate RB1. Taken

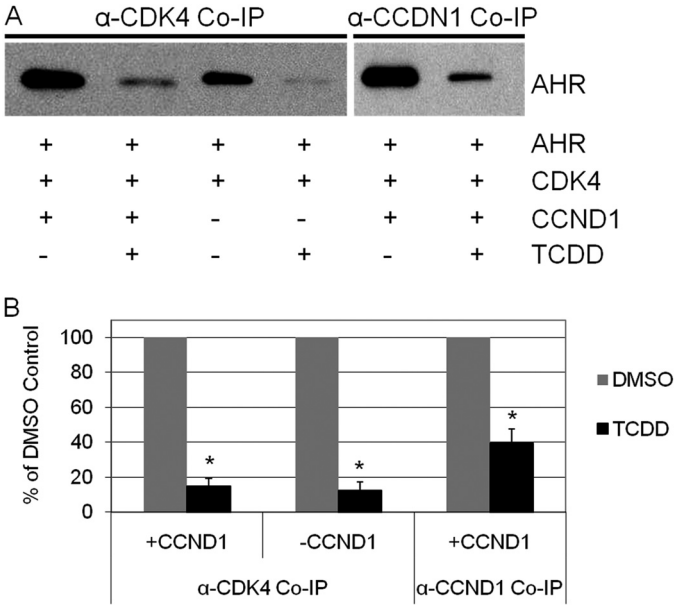

Fig. 5. Formation of the AHR/CDK4/CCND1 complex is disrupted by TCDD in vitro. AHR, CDK4, and CCND1 were in vitro-translated and allowed to form complexes in the presence or absence of 10 nM TCDD or 0.1% DMSO vehicle control. A, the protein complexes were pulled down with α-CDK4 or α-cyclin D1 agarose-conjugated beads and analyzed by SDS-PAGE and Western blotting. The results are representative of three independent experiments. B, densiometric measurements were normalized as a percentage of the DMSO vehicle control. The results are mean ± S.D. from three separate experiments. *, $p < 0.05$ based on a one-sample Student's t test.

together, these results suggest that the AHR may act as a scaffolding protein and may aid in the recruitment of RB1 to the AHR/CDK4/CCND1 complex (Fig. 7). The recruitment of RB1 allows its phosphorylation by CDK4 and facilitates cell cycle progression.

Upon exposure to the exogenous ligand TCDD, the interaction between the AHR and CDK4 is inhibited, and the temporal nature of the inhibition correlates with decreased RB1 phosphorylation and G_1 cell cycle arrest. In the biochemical reconstitution assays, exposure to the exogenous ligand TCDD caused the AHR to dissociate from CDK4 and CCND1, and the phosphorylation of RB1 was inhibited (Fig. 7). Based on previous studies, the ligand-bound receptor would subsequently bind to hypophosphorylated RB1, leading to the inhibition of EP300 recruitment (Marlowe et al., 2004). This assembly of proteins at E2F-responsive promoters leads to the repression of S-phase genes aiding in G_1 arrest. The ligand-bound AHR would also bind to ARNT and would promote transcription of the cell cycle inhibitor CDKN1B (p27Kip1) (Kolluri et al., 1999). The combination of these events would result in G_1 cell cycle arrest.

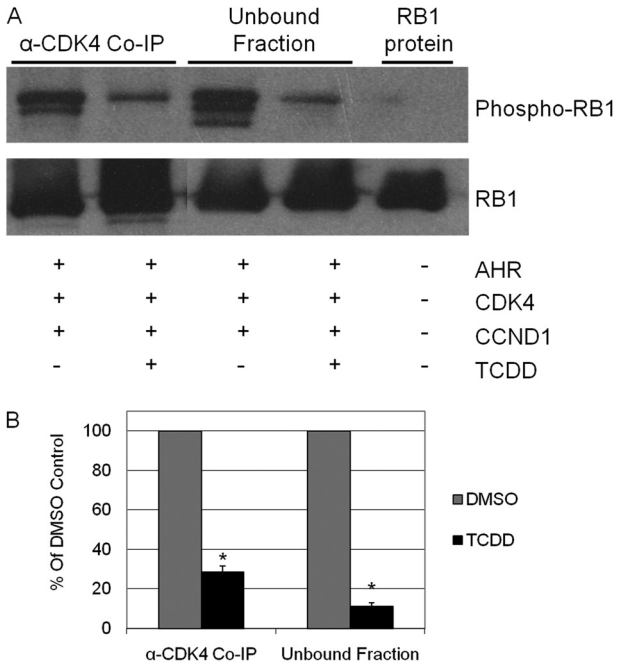

Fig. 6. CDK4 kinase activity by the AHR/CDK4/CCND1 complex is inhibited by TCDD in vitro. AHR, CDK4, and CCND1 were in vitro-translated and allowed to form complexes. After overnight coimmunoprecipitation with α-CDK4 agarose-conjugated beads, recombinant RB1 protein, 10 nM TCDD, or 0.1% DMSO vehicle control, kinase buffer, and ATP were added and allowed to incubate at 30°C for 30 min with shaking. A, the protein complexes were washed, eluted, and analyzed by SDS-PAGE and Western blotting. The results show a representative of three separate experiments. B, densiometric measurements were normalized as a percentage of the DMSO vehicle control. The results are mean ± S.D. from three separate experiments. *, $p < 0.05$ based on a one-sample Student's t test.

The role of an endogenous ligand for AHR in this process is unknown. In cells treated with only the vehicle, the AHR bound with CDK4 to facilitate RB1 phosphorylation and cell cycle progression. The interaction between AHR and CDK4 was replicated in reticulocyte lysate translations. If an endogenous ligand was present in both systems, it is clear that it is either required for the interaction to occur or at least does not hinder the process.

Although the present study expands the role for the AHR in cell cycle regulation, there are conflicting studies in the literature on the role of the receptor in the cell cycle. For example, one study reported that treatment of MCF-7 cells with TCDD did not induce G_1 cell cycle arrest and that knockdown of the AHR using RNA interference resulted in increased G_0/G_1 to S phase progression (Abdelrahim et al., 2003). This study is inconsistent with our results; however, there are several methodological and technical issues that hinder a direct comparison. First, the previous study used serum-free conditions after synchronization, which would keep the cells in growth arrest. In our study, cells were released from growth arrest with 8% charcoal-dextran-stripped FBS in the media after synchronization. Second, the previous study was performed in duplicate and only observed less than a 2% change in the percentage of cells in G_0/G_1 after treatment with TCDD and a 5% change in the percentage of cells in G_0/G_1 after knockdown of the AHR. This is signifi-

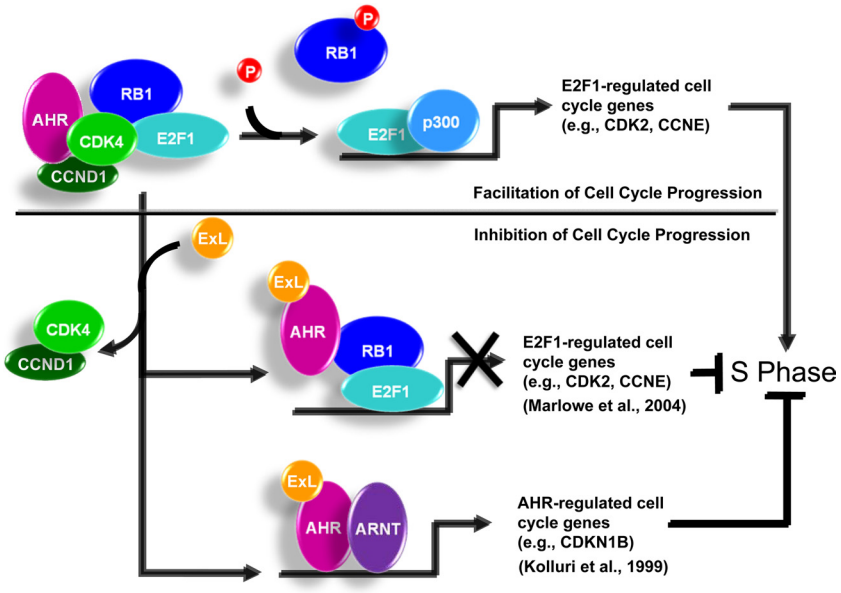

Fig. 7. Conceptual model of the role of the AHR in cell cycle regulation. The proposed model depicts the dual role of the AHR in both facilitating and inhibiting cell cycle progression based on both the present investigation and previous studies (Kolluri et al., 1999; Marlowe et al., 2004). In the absence of an exogenous ligand (ExL), the AHR assists in the formation of the CDK4/CCND1/RB1 complex, leading to RB1 hyperphosphorylation and cell cycle progression. On the other hand, in the presence of an exogenous ligand, such as TCDD, a conformation change in the AHR causes it to dissociate from CDK4/CCND1 and bind to the hypophosphorylated RB1 (Marlowe et al., 2004). The AHR/RB1 complex prevents the recruitment of EP300 inhibiting the expression of S-phase-dependent E2F1-regulated genes, such as CDK2 and CCNE (cyclin E). In addition, ligand-bound AHR also binds ARNT and promotes the transcription of the cell cycle inhibitor CDKN1B (p27Kip1) (Kolluri et al., 1999).

cantly smaller than the differences observed in our study and is consistent with a lack of growth release after synchronization. The study also did not include validation with a second, independent small interfering RNA duplex to eliminate the possibility of off-target effects (Jackson et al., 2003). Nonetheless, our results are consistent with a separate study using MCF-7 cells and similar synchronization methods that showed a 15 to 20% increase in the percentage of cells in G_1 after treatment with TCDD (Marlowe et al., 2004).

In summary, we have demonstrated a functional interaction between the AHR and CDK4 in both ER− and ER+ human breast cancer cell lines that allows the receptor to function as a molecular switch within the cell cycle. This switch-like function is compatible with the existing model of the role of the AHR in the cell cycle while extending the model to provide a mechanism by which the receptor can also facilitate cell cycle progression. Within mammary epithelial cells, the integrated model can explain both the lack of mammary development in the AHR knockout mice, in which facilitation of cell cycle progression by the receptor is absent (Hushka et al., 1998), as well as the epidemiological and rodent data demonstrating the inhibition of mammary tumorigenesis by exogenous AHR ligands (Bertazzi et al., 1997; National Toxicology Program, 2006; Viel et al., 2008).

References

Abdelrahim M, Smith R 3rd, and Safe S (2003) Aryl hydrocarbon receptor gene silencing with small inhibitory RNA differentially modulates Ah-responsiveness in MCF-7 and HepG2 cancer cells. *Mol Pharmacol* **63:**1373–1381.

Bertazzi PA, Zocchetti C, Guercilena S, Consonni D, Tironi A, Landi MT, and Pesatori AC (1997) Dioxin exposure and cancer risk: a 15-year mortality study after the "Seveso accident". *Epidemiology* **8:**646–652.

Bunger MK, Glover E, Moran SM, Walisser JA, Lahvis GP, Hsu EL, and Bradfield CA (2008) Abnormal liver development and resistance to 2,3,7,8-tetrachlorodibenzo-p-dioxin toxicity in mice carrying a mutation in the DNA-binding domain of the aryl hydrocarbon receptor. *Toxicol Sci* **106:**83–92.

Dong B and Matsumura F (2009) The conversion of rapid TCCD nongenomic signals to persistent inflammatory effects via select protein kinases in MCF10A cells. *Mol Endocrinol* **23:**549–558.

Elferink CJ, Ge NL, and Levine A (2001) Maximal aryl hydrocarbon receptor activity depends on an interaction with the retinoblastoma protein. *Mol Pharmacol* **59:** 664–673.

Flemington EK, Speck SH, and Kaelin WG Jr (1993) E2F-1-mediated transactivation is inhibited by complex formation with the retinoblastoma susceptibility gene product. *Proc Natl Acad Sci U S A* **90:**6914–6918.

Ge NL and Elferink CJ(1998) A direct interaction between the aryl hydrocarbon receptor and retinoblastoma protein. Linking dioxin signaling to the cell cycle. *J Biol Chem* **273:**22708–22713.

Haarmann-Stemmann T, Bothe H, and Abel J (2009) Growth factors, cytokines and their receptors as downstream targets of arylhydrocarbon receptor (AhR) signaling pathways. *Biochem Pharmacol* **77:**508–520.

Hahn ME, Allan LL, and Sherr DH (2009) Regulation of constitutive and inducible AHR signaling: complex interactions involving the AHR repressor. *Biochem Pharmacol* **77:**485–497.

Hankinson O (1995) The aryl hydrocarbon receptor complex. *Annu Rev Pharmacol Toxicol* **35:**307–340.

Hsu EL, Yoon D, Choi HH, Wang F, Taylor RT, Chen N, Zhang R, and Hankinson O (2007) A proposed mechanism for the protective effect of dioxin against breast cancer. *Toxicol Sci* **98:**436–444.

Hushka DR and Greenlee WF (1995) 2,3,7,8-Tetrachlorodibenzo-p-dioxin inhibits DNA synthesis in rat primary hepatocytes. *Mutat Res* **333:**89–99.

Hushka LJ, Williams JS, and Greenlee WF (1998) Characterization of 2,3,7,8-tetrachlorodibenzofuran-dependent suppression and AH receptor pathway gene expression in the developing mouse mammary gland. *Toxicol Appl Pharmacol* **152:**200–210.

Jackson AL, Bartz SR, Schelter J, Kobayashi SV, Burchard J, Mao M, Li B, Cavet G, and Linsley PS (2003) Expression profiling reveals off-target gene regulation by RNAi. *Nat Biotechnol* **21:**635–637.

Kato J, Matsushime H, Hiebert SW, Ewen ME, and Sherr CJ (1993) Direct binding of cyclin D to the retinoblastoma gene product (pRb) and pRb phosphorylation by the cyclin D-dependent kinase CDK4. *Genes Dev* **7:**331–342.

Kolluri SK, Weiss C, Koff A, and Göttlicher M (1999) p27(Kip1) induction and inhibition of proliferation by the intracellular Ah receptor in developing thymus and hepatoma cells. *Genes Dev* **13:**1742–1753.

Ma Q and Whitlock JP Jr (1996) The aromatic hydrocarbon receptor modulates the Hepa 1c1c7 cell cycle and differentiated state independently of dioxin. *Mol Cell Biol* **16:**2144–2150.

Marlowe JL, Knudsen ES, Schwemberger S, and Puga A (2004) The aryl hydrocarbon receptor displaces p300 from E2F-dependent promoters and represses S phase-specific gene expression. *J Biol Chem* **279:**29013–29022.

Marlowe JL and Puga A (2005) Aryl hydrocarbon receptor, cell cycle regulation, toxicity, and tumorigenesis. *J Cell Biochem* **96:**1174–1184.

National Toxicology Program (2006) NTP technical report on the toxicology and carcinogenesis studies of 2,3,7,8-tetrachlorodibenzo-p-dioxin (TCDD) (CAS No. 1746-01-6) in female Harlan Sprague-Dawley rats (Gavage Studies). *Natl Toxicol Program Tech Rep Ser* **(521):**4–232.

Ohtake F, Fujii-Kuriyama Y, and Kato S (2009) AhR acts as an E3 ubiquitin ligase to modulate steroid receptor functions. *Biochem Pharmacol* **77:**474–484.

Patel RD, Murray IA, Flaveny CA, Kusnadi A, and Perdew GH (2009) Ah receptor represses acute-phase response gene expression without binding to its cognate response element. *Lab Invest* **89:**695–707.

Petrulis JR and Perdew GH (2002) The role of chaperone proteins in the aryl hydrocarbon receptor core complex. *Chem Biol Interact* **141:**25–40.

Poland A and Knutson JC (1982) 2,3,7,8-tetrachlorodibenzo-p-dioxin and related halogenated aromatic hydrocarbons: examination of the mechanism of toxicity. *Annu Rev Pharmacol Toxicol* **22:**517–554.

Puga A, Barnes SJ, Dalton TP, Chang C, Knudsen ES, and Maier MA (2000) Aromatic hydrocarbon receptor interaction with the retinoblastoma protein potentiates repression of E2F-dependent transcription and cell cycle arrest. *J Biol Chem* **275:**2943–2950.

Ray S and Swanson HI (2009) Activation of the aryl hydrocarbon receptor by TCDD inhibits senescence: a tumor promoting event? *Biochem Pharmacol* **77:**681–688.

Tan Z, Chang X, Puga A, and Xia Y (2002) Activation of mitogen-activated protein kinases (MAPKs) by aromatic hydrocarbons: role in the regulation of aryl hydrocarbon receptor (AHR) function. *Biochem Pharmacol* **64:**771–780.

Thomsen JS, Kietz S, Ström A, and Gustafsson JA (2004) HES-1, a novel target gene for the aryl hydrocarbon receptor. *Mol Pharmacol* **65:**165–171.

Viel JF, Clément MC, Hägi M, Grandjean S, Challier B, and Danzon A (2008) Dioxin emissions from a municipal solid waste incinerator and risk of invasive breast cancer: a population-based case-control study with GIS-derived exposure. *Int J Health Geogr* **7:**4.

Wang W, Smith R 3rd, and Safe S (1998) Aryl hydrocarbon receptor-mediated antiestrogenicity in MCF-7 cells: modulation of hormone-induced cell cycle enzymes. *Arch Biochem Biophys* **356:**239–248.

Weiss C, Kolluri SK, Kiefer F, and Göttlicher M (1996) Complementation of Ah receptor deficiency in hepatoma cells: negative feedback regulation and cell cycle control by the Ah receptor. *Exp Cell Res* **226:**154–163.

Wormke M, Stoner M, Saville B, Walker K, Abdelrahim M, Burghardt R, and Safe S (2003) The aryl hydrocarbon receptor mediates degradation of estrogen receptor alpha through activation of proteasomes. *Mol Cell Biol* **23:**1843–1855.

Address correspondence to: Dr. Russell S. Thomas, The Hamner Institutes for Health Sciences, 6 Davis Drive, P.O. Box 12137, Research Triangle Park, NC 27709. E-mail: rthomas@thehamner.org